3-3 A Strontium Optical Lattice Clock

YAMAGUCHI Atsushi, SHIGA Nobuyasu, NAGANO Shigeo, ISHIJIMA Hiroshi, KOYAMA Yasuhiro, HOSOKAWA Mizuhiko, and IDO Tetsuya

Atomic frequency standards project started to build a Strontium (Sr) optical lattice clock in 2006. We have recently trapped laser cooled Sr atoms in a 1D optical lattice potential and carried out spectroscopy of the clock transition with the linewidth of 45 Hz. We have also stabilized the clock laser frequency to the clock transition. The stability of our lattice clock compared with our hydrogen maser is limited by the stability of the hydrogen maser, which means that our lattice clock is much more stable than the hydrogen maser.

Keywords
Optical frequency standard, Optical lattice clock, Laser cooling and trapping

1 Introduction

Frequency standards not only play a prominent part in social life in general, including GPS, but also as an essential part of studies in fundamental physics. At present, the atomic clock using cesium atoms serves the role of the primary standard for defining one second. As an optical frequency standard capable of realizing accuracy and stability far beyond this, Katori proposed the idea of the "optical lattice clock" in 2001[1][2]. In this report we will first provide a brief introduction of the principle of optical lattice clocks and then describe our experiments.

1.1 Principle of optical lattice clock

Researches of optical frequency standards aim for precise measurement of the unperturbed resonance frequency of the forbidden atomic transition (clock transition) through laser spectroscopy. The natural linewidth of the clock transition is normally 1 to 10 mHz. When conducting precise spectroscopy of the clock transition, Doppler broadening becomes the first issue. Even if atoms moving in free space can be cooled to as far as 1 μK, a typical temperature attainable by laser cooling, a Doppler broadening of tens of kHz remains. In order to suppress the Doppler broadening, it is necessary to tightly confine atoms in a trap and prevent them from moving to the probe laser as little as possible. It is known that if atoms are confined in the spatial region whose scale is smaller than the wavelength of the probe laser, Doppler broadening can be eliminated (Lamb-Dicke confinement)[3][4]. This condition can be quantitatively expressed by the Lamb-Dicke parameter η, which is defined as follows[5]:

$$\eta = \frac{2\pi x_0}{\lambda_{\mathrm{clock}}} \tag{1}$$

In this equation, x_0 stands for the width of spatial distribution of atoms in the trap, and λ_{clock} for the wavelength of the probe laser. Therefore, how much the Lamb-Dicke confinement is realized can be quantitatively expressed by how much x_0 is smaller than λ_{clock} or how much η is smaller than 1.

The optical lattice clock achieves the Lamb-Dicke confinement by trapping atoms in an optical lattice potential which is a periodic potential generated by standing waves of laser

light. Consider Strontium (Sr) atoms used for the experiment described in this paper as an example. The wavelength of the probe laser is (λ_{clock}=) 698 nm. For the optical lattice potential, meanwhile, a laser with the wavelength of 813 nm is used for the reason to be mentioned below. Atoms are strongly confined at the antinode of standing waves which are lining up at an interval of 407 nm, i.e. half the wavelength of optical lattice laser. As the result, x_0 is approximately 30 nm. Therefore, the Lamb-Dicke parameter η becomes 0.3 (< 1) and the Lamb-Dicke confinement is achieved.

The next issue is the Stark shift due to the trap laser. When atoms are trapped in an optical lattice potential, each energy level of the atoms shifts depending on the wavelength and intensity of the trap laser (Stark shift). In general, the Stark shift of the ground state is different from that of the excited state, which leads to the shift of the resonance frequency of the clock transition. However, if a particular wavelength is selected, the Stark shifts due to the trap laser become exactly the same between the ground and excited states[6]. In other words, the resonance frequency of the clock transition does not shift even though atoms are trapped in an optical lattice potential. This wavelength is called the magic wavelength, which has been experimentally measured to be 813.428 nm in case of Sr[2]. Therefore, if atoms are trapped in the optical lattice potential at the magic wavelength, we can eliminate the Doppler broadening by the Lamb-Dicke confinement without affecting the clock transition. Furthermore, the optical lattice clock can trap multiple atoms (approximately 10^3–10^4) at a time. A significant improvement of S/N ratio is hence promising compared with the ion trap that continues to observe a single ion, and it is supposedly possible to create an ultrahigh-precision frequency standard whose stability reaches 10^{-18} at an averaging time of one second.

1.2 Current situation of the optical lattice clock

The performance of the optical lattice clock using Sr atoms has been greatly investigated in a past several years[7]-[9]. The fermionic isotope ^{87}Sr has some advantages due to: its weakly allowed transition which is essentially forbidden can be used as the clock transition[10], and interatomic collisions with the same spin component are forbidden from statistical properties at an ultralow temperature, which leads to suppression of collisional shifts. The optical lattice clock using polarized fermionic isotopes was realized by the University of Tokyo, the NIST (USA), the SYRTE (France); the absolute frequencies from these three institutes were confirmed to be equal within the range of error. In 2006, the resonance frequency of the clock transition in the fermionic isotope ^{87}Sr was listed as a secondary representation of the second.

2 Laser cooling of strontium atoms

The potential depth of an optical lattice potential is approximately 15 μK in terms of temperature. We thus have to cool Sr atoms down to a temperature lower than the potential depth to trap them in the optical lattice potential.

Strontium is an alkaline-earth metal with atomic number 38. It has two valence electrons in the outermost shell (so-called two-electron system), and there exist the spin singlet and triplet states on the energy levels. Figure 1 shows energy levels relating to our experiment. $^1S_0$ denotes the ground state. The $^1S_0$–$^1P_1$ transition (wavelength: 461 nm, natural linewidth: 32 MHz, Doppler limit temperature: 720 μK) is the strongest transition from the ground state, and used as the transition for deceleration of

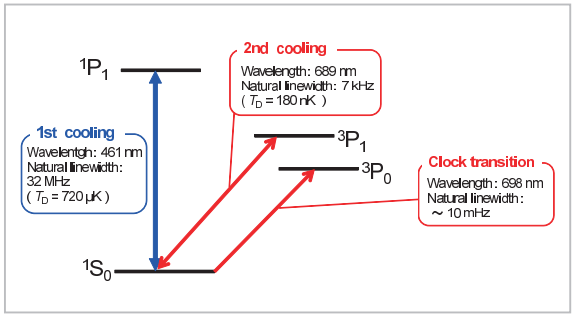

Fig.1 *Energy levels of Sr atoms*

atomic beams and the 1st stage magneto-optical trap (MOT). MOT is a method for cooling and trapping atoms spatially by laser irradiation from six directions to atoms in the magnetic gradient. The narrower the natural linewidth of the optical transition for use is, the lower the attainable temperature (Doppler limit temperature) becomes. Therefore, we first decelerated atoms, cooled and trapped as many atoms as possible by using a large radiation pressure of the strong transition ($^1S_0$–$^1P_1$). Having then switched to MOT using the transition with a narrower natural linewidth ($^1S_0$–$^3P_1$), we cooled atoms down to the temperature which is well lower than the trap depth of the optical lattice potential.

Here, we describe the experimental procedure (ref. Fig. 2). First, we vaporize Sr atoms in an oven at 600 ºC to generate an atomic beam. Next, we irradiate this atomic beam with the laser, whose frequency is slightly lower than the strong $^1S_0$–$^1P_1$ transition, from the opposite direction to decelerate the atomic beam by its strong radiation force. The slight lowering of frequency is intended to compensate for the Doppler shift. Additionally, by the magnetic field gradient from the oven to the trap chamber, we compensate with the Zeeman shift for changes in the Doppler shift owing to deceleration so that the deceleration laser can always resonate with atoms (Zeeman slowing technique). The atoms reach the center of the trap chamber and are trapped by MOT. In our experiment, the atoms are first trapped in MOT using the strong $^1S_0$–$^1P_1$ transition, and approximately 10^7 atoms are cooled down to 2 mK. In order to further cool these atoms, they are transferred to MOT using the weak $^1S_0$–$^3P_1$ transition (wavelength: 689 nm, natural linewidth: 7 kHz, Doppler limit temperature: 180 nK). The atoms are then cooled down to 3 μK[11]. By overlapping the optical lattice laser with a trap depth of 15 μK onto this atomic cloud, the atoms are trapped in the optical lattice potential (see Fig. 3). According to the above described procedure, our experiment has succeeded in trapping approximately 10^4 ^{87}Sr atoms in the optical lattice potential.

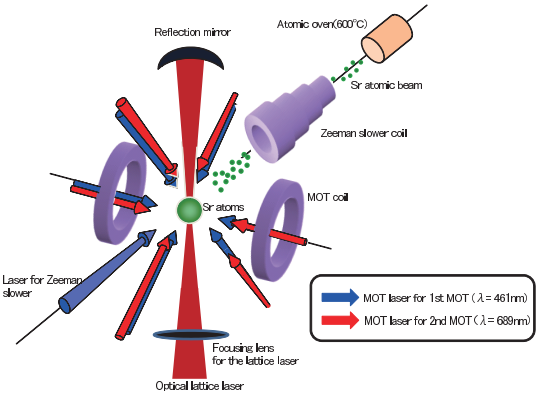

Fig.2 *Experiment system for laser cooling of Sr atoms*

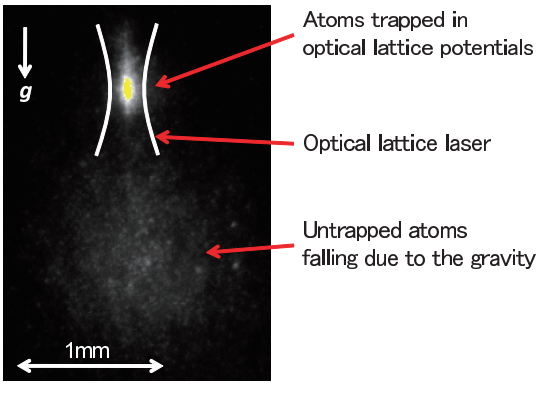

Fig.3 *CCD Image of ^{87}Sr atoms trapped in the optical lattice potential*

Here, we provide a brief description of each laser source that is used for laser cooling. The laser (461 nm) for deceleration of the atomic beam and for the 1st MOT is obtained by amplifying the laser diode (LD) output (922 nm) with the tapered amplifier and converting wavelength with nonlinear crystal $KNbO_3$. We carry out the saturated absorption spectroscopy of the $^1S_0$–$^1P_1$ transition of ^{88}Sr atoms (bosonic isotope with the highest natural abundance) in a galvanic cell and generate error signals via the FM spectroscopy for frequency stabilization. Laser power is 30 mW for MOT (prior to dividing into three axes) and 25 mW for Zeeman slowing. The beam radius and detuning of MOT light are 1 cm and 40 MHz respectively, and the MOT magnetic gradient is 65 Gauss/cm (in the direction of the central axis of coil). The

detuning of Zeeman slowing light is 760 MHz. LD is used for the 2nd MOT (689 nm). First, we stabilize the master laser frequency to the cavity with a fineness of 150,000. Next, we combine the saturated absorption spectroscopy with the FM spectroscopy to stabilize the laser frequency to the $^1S_0$–$^3P_1$ transition (m = 0) of ^{88}Sr atoms. For MOT, we use 5 mW (prior to dividing into three axes) from the slave laser whose frequency is phase-locked to the master laser. The MOT magnetic gradient is 8 Gauss/cm (in the direction of the central axis of coil). As the optical lattice laser, the Ti: sapphire laser with a magic wavelength of 813.428 nm is used with the 320 mW power and a beam radius of 30 μm at the position of atomic cloud.

3 Clock laser

Next, we give an explanation of the laser for excitation of the clock transition (clock laser). The wavelength of the clock transition $^1S_0$–$^3P_0$ in Sr atoms is 698 nm, which can be generated by LD. Figure 4 shows the overview of the system for the clock laser stabilization developed in our experiment.

The LD frequency is first stabilized to the prestabilization cavity (F=5,200) by the Pound-Drever-Hall technique[12]. The prestabilization cavity is composed of a 10 cm cylinder made from super invar, and a PZT and a mirror attached to the both sides of the cylinder. The laser frequency is then stabilized to the high finesse cavity (F=200,000) made of the ultralow expansion (ULE) glass by the Pound-Drever-Hall technique. The ULE cavity is a cylinder with 10 cm length and 5 cm diameter and laid down being supported by four points that are insensitive to vibration from the floor. The bandwidth of the locking circuit is 2 MHz for the prestabilization cavity and 90 kHz for the stabilization to the ULE cavity. Temperature of the ULE cavity is precisely controlled and its fluctuation is suppressed to be ±500 μK or less per day. As a result, frequency drift of the laser stabilized to the ULE cavity is kept below 0.1 Hz/s. The ULE cavity is put in the vacuum chamber to suppress the frequency fluctuations due to the air flow. The vacuum chamber is placed on the high-performance vibration-free platform to suppress the effect of vibrations from the floor (Minus-K Technology, Inc., 150 MB-1, 0.5 Hz resonance frequency). Furthermore, the whole device is put in the soundproof box to avoid the impact of acoustic noise. For spectroscopy of the clock transition, we deliver the light to the trap chamber and to the optical frequency comb through optical fibers. Optical fibers of

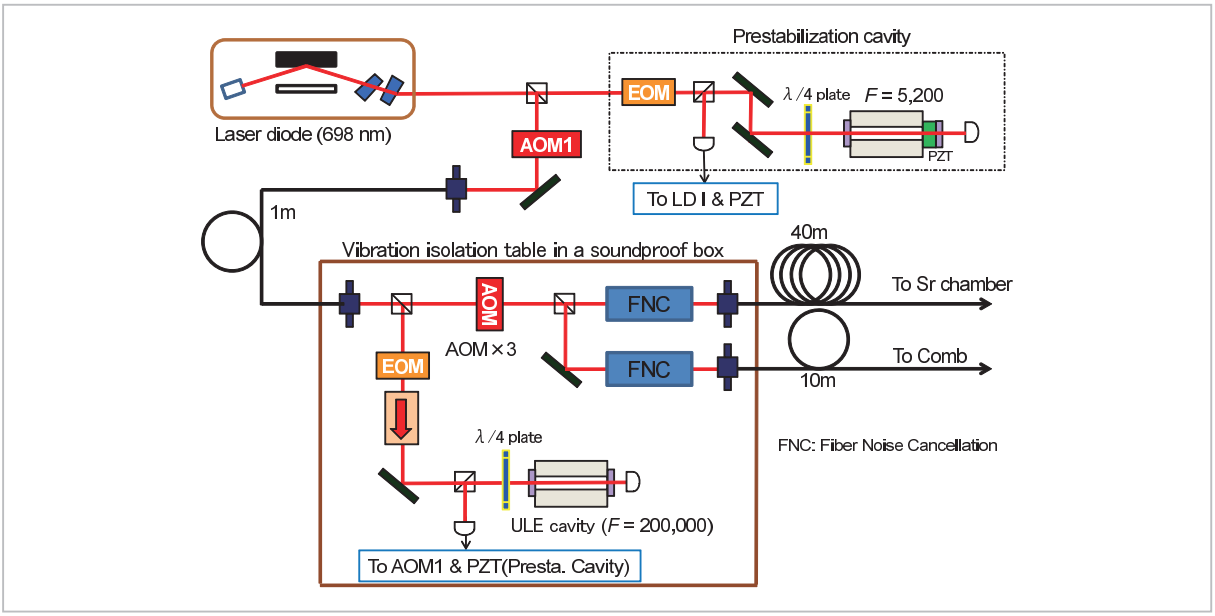

Fig.4 *Overall view of the system for Sr clock laser stabilization*

40 m and 10 m each are thereby used; in order to prevent the clock laser frequency from containing noise by using these optical fibers, the fiber noise cancellation schemes are introduced to each (FNC in Fig. 4).

Figure 5 shows the results of comparison in frequency stabilities between the clock laser used in our experiment (698 nm) and CSO (Cryogenic Sapphire Oscillator). CSO is an oscillator with superior short-term frequency stability. The black circles in Fig. 5 stand for the stability of CSO itself, and the red squares describe the stability between CSO and the clock laser which was measured via a frequency comb. Beat frequency was measured by a frequency counter (Agilent Technologies, Inc., 53181A). The fractional stability reached 4×10^{-15} at an averaging time of 20 seconds, which indicates that the present stability enables measurements of the clock transition frequency on the Hz level. However, the thermal noise of mirrors that is considered to determine the limit of the clock laser stability is at the level of 10^{-16}. Therefore, we are still improving the device aiming at further improvement of stability.

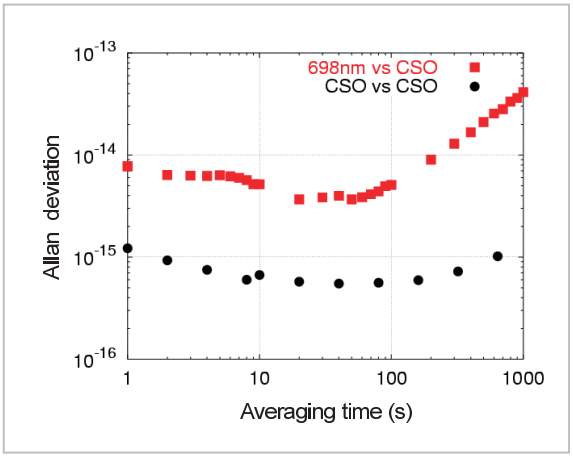

Fig.5 *Comparison between clock laser (698 nm) and CSO in stabilization*

4 Spectroscopy of clock transition

In the above, we described ^{87}Sr atoms trapped in the optical lattice potential and the stable clock laser to observe its clock transition. In the following, we discuss the spectroscopy for the $^1S_0$–$^3P_0$ clock transition of ^{87}Sr atoms.

4.1 Normalization of the number of excited atoms

In our experiment, we normalize the number of excited atoms to evaluate the excitation efficiency of the clock transition. Figure 6 shows its outline.

(Step 1) First, we irradiate ^{87}Sr atoms in the optical lattice potential with the clock laser. If

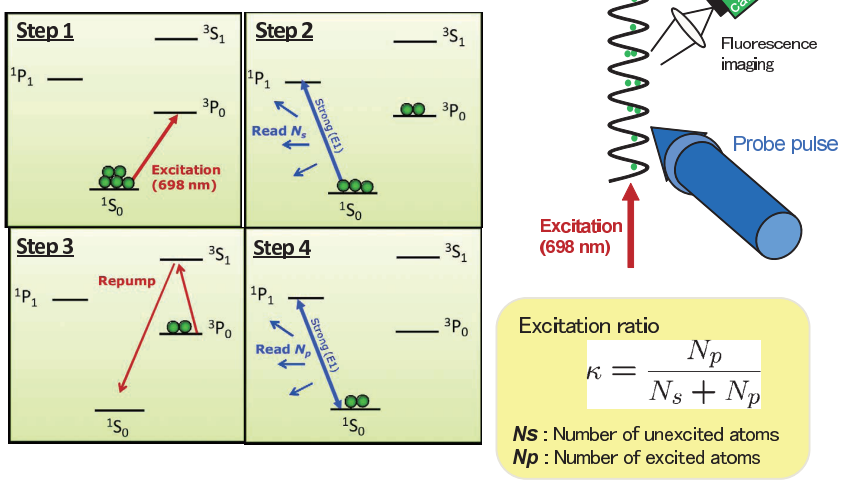

Fig.6 *Evaluation method for excitation efficiency through standardization of the number of atoms*

the clock laser frequency is resonant with the clock transition, some atoms are excited. We can consider that once excited, atoms will remain in the excited state since the lifetime of the exited state is 150s while Steps 1–4 end in 100 ms or shorter.

(Step 2) Next, we irradiate atoms with the laser which is resonant with the strong $^1S_0$–$^1P_1$ transition and then observe the emission intensity with a CCD camera. From this emission intensity, we can evaluate the number of atoms remaining unexcited (Ns). Through this operation, the atoms remaining in the ground state are heated and blown away from the optical lattice potential.

(Step 3) We return the atoms that have been excited in Step 1 to the ground state with the repump laser.

(Step 4) Again, we irradiate atoms with the laser which is resonant with the strong $^1S_0$–$^1P_1$ transition. From the emission intensity at this time, we can evaluate the number of atoms excited in Step 1 (Np).

From the above procedure, we are able to calculate the excitation efficiency of the clock transition: $\kappa = N\mathrm{p}/(N\mathrm{s}+N\mathrm{p})$. The advantage of this method is that the excitation efficiency κ can be evaluated without being affected by fluctuations of the initial atom number (Ns+Np). It is also possible to observe the clock transition by seeing the change of emission intensity in only Step 2 as changing the clock laser frequency. In this case, however, it is indistinguishable whether the reduction of emission intensity is caused by the reduction of initial atom number or by the clock transition, which eventually leads to the degradation of S/N ratio.

It takes three seconds for one cycle of the spectroscopy: the 1st MOT → the 2nd MOT → loading atoms into the optical lattice potential → excitation of the clock transition → normalization of the number of excited atoms. Repeating this cycle while changing the clock laser frequency and observing changes of excitation efficiency κ, we are performing the clock transition spectroscopy.

4.2 Observation of sideband spectrum

Next, using the clock transition, we experimentally evaluated the confinement of the optical lattice potential and the temperature of trapped atoms[5]. Figure 7 shows the results; the horizontal axis represents the clock laser frequency (laser detuning), and the vertical axis the excitation efficiency κ of the clock transition (excitation fraction). The origin of the horizontal axis corresponds to the resonance frequency of the clock transition. In addition to the carrier spectrum, two sidebands (red sideband and blue sideband) are observed. These two sidebands can be explained in the

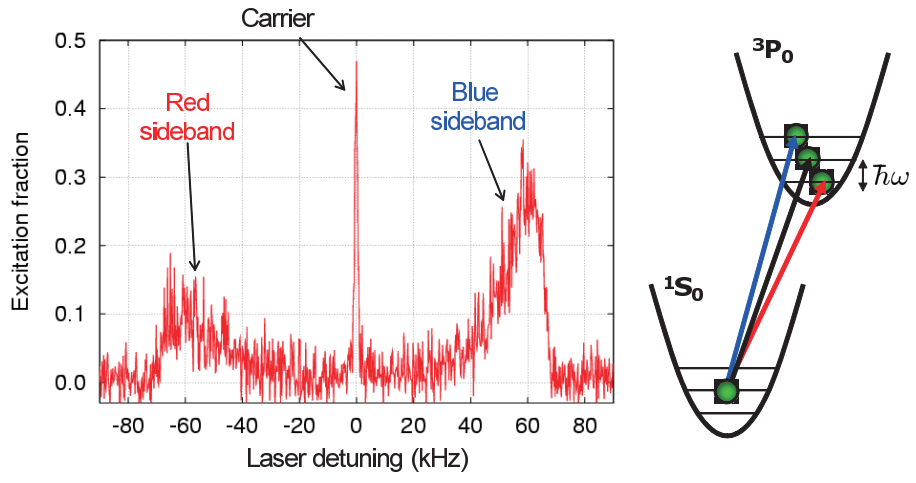

Fig.7 *Observation of the sideband spectrum of the optical lattice potential*

following way.

The optical lattice potential can be well approximated by the harmonic oscillator potential. Hence, when the vibrational frequency of the trap is set as ω, energy levels (vibrational level) are lining at a constant interval of $\hbar\omega$ in ascending order: $|g, 0>, |g, 1>, \ldots |g, n>$. In this expression, the first character denotes the atomic state (g = ground state, e = excited state), and the second one the number of vibrational level. $\hbar$ denotes the values of Planck constant h divided by 2π. Now, since the optical lattice laser with magic wavelength is used, the vibrational frequency of the excited state is the same ω, and the vibrational levels are also lining at the same interval $\hbar\omega$ in ascending order: $|e, 0>, |e, 1>, \ldots |e, m>$. The trapped atoms are distributed to vibrational levels of the ground state, reflecting its temperature ($|g, 0>, |g, 1>$, ...). Probabilities of being excited from there to the vibrational level of the excited state can be calculated from the overlap of the wavefunction, and transition probabilities to the vibrational level with the same number become highest. Therefore, what most probably takes place is the transition: $|g, 0> \rightarrow |e, 0>, |g, 1> \rightarrow |e, 1>, \ldots$. Since these transition frequencies are all the same with use of the magic wavelength, they are observed as a sharp peak (carrier) such as near 0 Hz in Fig. 7. The second-probable transition is one whose vibrational levels shift by one such as: $|g, 0> \rightarrow |e, 1>, |g, 1> \rightarrow |e, 2> \ldots$ or $|g, 1> \rightarrow |e, 0>, |g, 2> \rightarrow |e, 1>$. The resonance frequency is shifted from the carrier by $\hbar\omega$ (one vibrational level). Here, the transition with a vibrational level higher by one level is called the blue sideband because of its high frequency, and that with a vibrational level lower by one level the red sideband because of its low frequency, which are observed on the both sides of the carrier as shown in Fig. 7. The interval between the carrier and the sidebands reflects the interval of the vibrational levels of the lattice potential. The vibrational frequency of the optical lattice potential, therefore, turns out $2\pi \times 60$ kHz from the spectrum in Fig. 7. Meanwhile, without going into detail, the reason why the spectral width of the sideband is wider against the carrier is that we use the one-dimensional optical lattice potential in our experiment.

Once vibrational frequency ω is evaluated, the confinement of the optical lattice potential or the before-mentioned Lamb-Dicke parameter η can be evaluated. Using Equation (1) with a modification, η can be expressed by using the vibrational frequency of the trap as follows:

$$\eta = \sqrt{\frac{\omega_R}{\omega}}$$

In this expression, ω_R denotes the recoil frequency due to the clock laser. Recoil frequency ω_R is $\hbar k^2/(2m)$ (k = wavenumber of the clock laser, m = mass of a strontium atom), leading to $2\pi \times 4.68$ kHz for 698 nm. Calculation from the trap frequency in our experiment derives $\eta = 0.28$, which is sufficiently smaller than 1. Thus the condition of Lamb-Dicke confinement is satisfied.

Moreover, from the spectrum in Fig. 7, the atomic temperature in the optical lattice potential can also be evaluated. The lower the temperature of atoms is, the more the number of atoms on the $|g, 0>$ vibrational level is. When atoms are excited from $|g, 0>$, there is no room for decrease in the value of the vibrational level because the atoms are already in the lowest vibrational level. In other words, the atoms make no more contribution to the red sideband. If one sees how much the red sideband is lower than the blue sideband, they notice how many atoms are in $|g, 0>$ or how much atoms are cooled. Having employed this method, we evaluated the atomic temperature as 3 μK from Fig. 7.

4.3 Stabilization of clock laser frequency to clock transition

The carrier spectrum in Fig. 7 is used for the clock operation since its frequency does not change even when atoms are trapped. Figure 8 shows the results for the precision spectroscopy of that carrier. The horizontal axis represents the clock laser frequency (setting the center of

observed resonance as 0 Hz), and the vertical axis the excitement efficiency. The observed spectral linewidth was 45 Hz. We believe that this width is limited by the Zeeman splitting of the hyperfine structure of the ground and excited states in a residual magnetic field.

Next, the clock laser frequency was stabilized to the center of this spectrum by the method shown in Fig. 9. We monitor the right and left side of the spectrum in Fig. 8 at its full width of half maximum and evaluate differences in its excitation efficiency. From these differences in excitation efficiency, we can calculate how much the center frequency is shifted. We then adjusted the clock laser frequency with AOM to correct such shifts. By applying this feedback continuously, the center frequency of the clock laser is stabilized to be always resonant with the clock transition. In our experiment, since it took three seconds for one cycle, feedback was applied every six seconds. We compared the clock laser stabilized in this manner with the hydrogen maser via an optical frequency comb. Specifically, we measured a beat signal between the comb stabilized to the hydrogen maser and the clock laser stabilized to the Sr clock transition by the zero dead-time frequency counter (Pendulum Instruments Inc., currently Spectracom Corp.). Figure 10 shows the results. The horizontal axis represents averaging time and the vertical one the Allan deviation. The observed Allan deviation is limited by the hydrogen maser, and thus the stability of the optical lattice clock in our experiment was confirmed to have a higher stability than the hydrogen maser. We are planning to evaluate the stability of our optical lattice clock by comparing with the calcium ion clock which is under development in our project, with CSO, or with the Sr lattice clock at the University of Tokyo via the fiberlink.

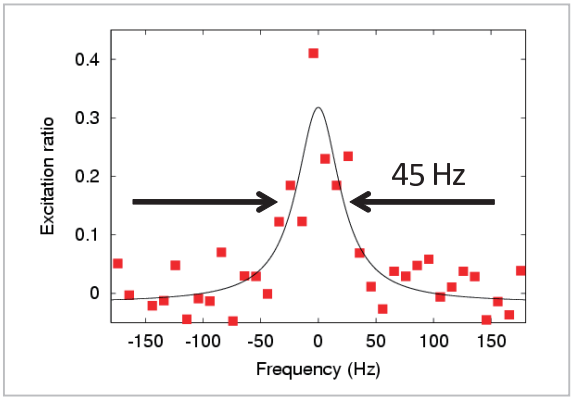

Fig.8 *Spectrum of the ^{87}Sr clock transition*

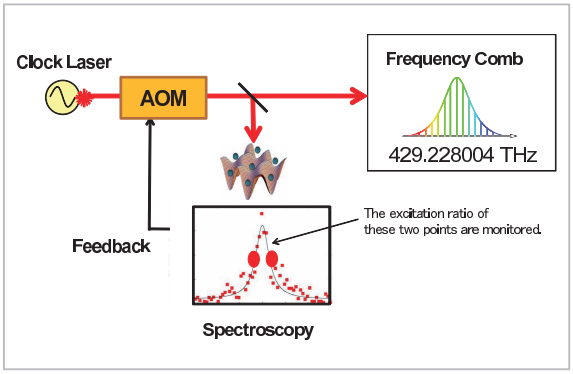

Fig.9 *Stabilization of clock laser frequency to clock transition*

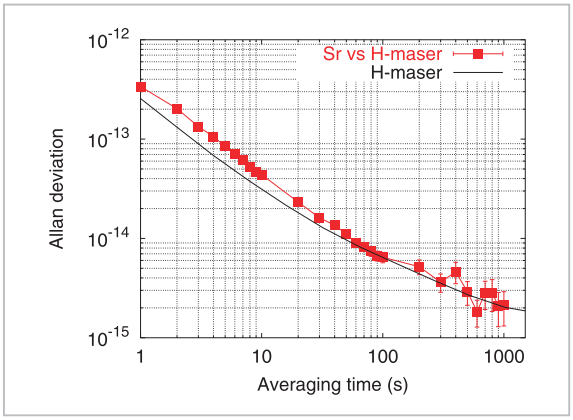

Fig.10 *Comparison between the clock laser stabilized to Sr clock transition and the hydrogen maser in stability*

5 Summary and future prospects

We succeeded in laser cooling the ^{87}Sr and trapping them in the optical lattice potential. Also, we developed the clock laser by which we observed the clock transition in ^{87}Sr with a linewidth of 45 Hz. Moreover, we successfully stabilized the clock laser frequency to the clock transition. Comparison between stabilities of this clock laser and the hydrogen maser using a frequency comb found that the stability was

limited by the hydrogen maser. In other words, it was confirmed that the optical lattice clock in our experiment far exceeded the hydrogen maser in stability.

For future prospects, one can expect performance advances in the clock laser. In our project, we are currently developing the optical cavity which has a low thermal noise of mirrors and insensitive to vibrations from the floor[13]. If this delivers the performance as is designed, the clock laser with the stability at the level of 10^{-16} will be realized. Regarding the optical lattice clock, we have considered that the existing spectrum is affected by the external magnetic field. To get rid of this difficulty, we plan to polarize atoms to the two stretched states of magnetic sublevels by use of the optical pumping technique and average the resonant frequencies of both spectra. Furthermore, in order to apply feedback to the clock laser frequency at a higher speed or minimize the cycle time, it is crucial to trap a higher number of atoms. It is also significant to attempt a direct comparison with the Sr optical lattice clock at the University of Tokyo, 24 km apart from NICT, using the fiberlink of the 1.5 μm communication band and accordingly detect the gravitational shift due to differences in elevation between the both. The difference in elevation between the University of Tokyo and NICT is 56 m, and thus the gravitational shift is predicted at 3.6 Hz. If the optical lattice clock at NICT attains an accuracy of $2\text{-}3\times10^{-15}$ in operation, the detection of the gravitational shift is feasible enough.

Acknowledgements

We would like to offer our heartfelt gratitude to Mr. Masatoshi Kajita, Mr. Motohiro Kumagai, Ms. Li Ying, Mr. Asahiko Nogami, Mr. C. R. Locke, Mr. J. G. Hartnett (The University of Western Australia) and Mr. G. Santarelli (SYRTE) for their untiring assistance while conducting the present research.

References

1 H. Katori, "Spectroscopy of strontium atoms in the Lamb-Dicke confinement," Proceedings of the 6th Symposium on Frequency Standards and Metrology, pp. 323–330, 2002.

2 Masao Takamoto, Feng-Lei Hong, Ryoichi Higashi, and Hidetoshi Katori, "An optical lattice clock," Nature, Vol. 435, pp. 321–324, 2005.

3 R. H. Dicke, "The Effect of Collisions upon the Doppler Width of Spectral Lines," Physical Review, Vol. 89, No. 2, pp. 472–473, 1953.

4 Masao Takamoto and Hidetoshi Katori, "Spectroscopy of the $^1S_0$–$^3P_0$ Clock Transition of ^{87}Sr in an Optical Lattice," Physical Review Letters, Vol. 91, No. 22, p. 223001, 2003.

5 D. J. Wineland and Wayne M. Itano, "Laser cooling of atoms," Physical Review A, Vol. 20, No. 4, pp. 1521–1540, 1979.

6 Hidetoshi Katori, Masao Takamoto, V. G. Pal'chikov, and V. D. Ovsiannikov, "Ultrastable Optical Clock with Neutral Atoms in an Engineered Light Shift Trap," Physical Review Letters, Vol. 91, No. 17, p. 173005, 2003.

7 Gretchen K Campbell, Andrew D Ludlow, Sebastian Blatt, Jan W Thomsen, Michael J Martin, Marcio H G de Miranda, Tanya Zelevinsky, Martin M Boyd, Jun Ye, Scott A Diddams, Thomas P Heavner, Thomas E Parker, and Steven R Jefferts, "The absolute frequency of the ^{87}Sr optical clock transition," Metrologia, Vol. 45, pp. 539–548, 2008.

8 X. Baillard, M. Fouche, R. Le Targat, P. G. Westergaard, A. Lecallier, F. Chapelet, M. Abgrall, G. D. Rovera, P. Laurent, P. Rosenbusch, S. Bize, G. Santarelli, A. Clairon, P. Lemonde, G. Grosche, B. Lipphardt,

and H. Schnatz, “An optical lattice clock with spin-polarized 87Sr atoms,” The European Physical Journal D, Vol. 48, pp. 11–17, 2008.

9 F.-L. Hong, M. Musha, M. Takamoto, H. Inaba, S. Yanagimachi, A. Takamizawa, K. Watabe, T. Ikegami, M. Imae, Y. Fujii, M. Amemiya, K. Nakagawa, K. Ueda, and H. Katori, “Measuring the frequency of a Sr optical lattice clock using a 120 km coherent optical transfer,” Optics Letters, Vol. 34, No. 5, pp. 692–694, 2009.

10 Sergey G. Porsev and Andrei Derevianko, “Hyperfine quenching of the metastable $^{3}P_{0,\,2}$ states in divalent atoms,” Physical Review A, Vol. 69, p. 042506, 2004.

11 Takashi Mukaiyama, Hidetoshi Katori, Tetsuya Ido, Ying Li, and Makoto Kuwata-Gonokami, “Recoil-Limited Laser Cooling of ^{87}Sr Atoms near the Fermi Temperature,” Physical Review Letters, Vol. 90, p. 113002, 2003.

12 R. W. P. Drever, J. L. Hall, F. V. Kowalski, J. Hough, G. M. Ford, A. J. Munley, and H. Ward, “Laser phase and frequency stabilization using an optical resonator,” Applied Physics B, Vol. 31, pp. 97–105, 1983.

13 Michi Koide and Tetsuya Ido, “Design of Monolithic Rectangular Cavity of 30-cm Length,” Japanese Journal of Applied Physics, Vol. 49, p. 060209, 2010.

(Accepted Oct. 28, 2010)

YAMAGUCHI Atsushi, *Ph.D.*
Expert Researcher, Space-Time Standards Group, New Generation Network Research Center
Atomic Frequency Standards

SHIGA Nobuyasu, *Ph.D.*
Guest Researcher, Space-Time Standards Group, New Generation Network Research Center
Atomic Frequency Standards

NAGANO Shigeo, *Ph.D.*
Senior Researcher, Space-Time Standards Group, New Generation Network Research Center
Optical Frequency Standards, Space-Time Measurements

ISHIJIMA Hiroshi
Technical Expert, Space-Time Standards Group, New Generation Network Research Center
Atomic Frequency Standards

KOYAMA Yasuhiro, *Ph.D.*
Group Leader, Space-Time Standards Group, New Generation Network Research Center
Space Geodesy, Radio Science

HOSOKAWA Mizuhiko, *Ph.D.*
Executive Director, New Generation Network Research Center
Atomic Frequency Standards, Space-Time Measurements

IDO Tetsuya, *Ph.D.*
Senior Researcher, Space-Time Standards Group, New Generation Network Research Center
Optical Frequency Standards, Optical Precision Measurement, Precision Transfer of Optical Frequency